ELSEVIER

Journal of Non-Crystalline Solids 250–252 (1999) 182–190

JOURNAL OF NON-CRYSTALLINE SOLIDS

www.elsevier.com/locate/jnoncrysol

Section 4. Liquid metals – clusters and surfaces

X-ray studies of liquid metal surfaces

H. Tostmann [a], E. DiMasi [b], B.M. Ocko [b], M. Deutsch [c], P.S. Pershan [a,*]

[a] *Division of Engineering and Applied Sciences, Harvard University, Cambridge, MA 02138, USA*
[b] *Department of Physics, Brookhaven National Laboratory, Upton, NY 11973-5000, USA*
[c] *Department of Physics, Bar-Ilan University, Ramat-Gan 52900, Israel*

Abstract

X-ray reflectivity and diffuse scattering measurements of the surface of liquid Hg, Ga and In are reviewed. For each metal surface induced layering is found. The surface structure of these metals is compared and differences are discussed in relation to bulk structural features such as the degree of covalency. Studies of modified liquid metal surfaces are also presented. The surface oxidation of liquid Ga, In and Hg is compared. Experimental results on surface segregation in Ga–In and Ga–Bi alloys and details of the surface wetting transition in Ga–Bi are also discussed.

1. Introduction

The structure of bulk liquid metals (LM) is not very different from the bulk structure of simple dielectric liquids [1]. The liquid structure factor and consequently the pair correlation function are virtually identical for liquid noble gases such as Ar and liquid alkali metals such as Cs [1]. This similarity indicates that the different interatomic interactions prevailing in these two classes of fluids do not affect the bulk structure. The atomic structure at liquid interfaces on the other hand, is very sensitive to the specific interactions [2]. At the surface of liquid metals for instance, the interactions change within a few atomic diameters from metallic in the liquid phase to van der Waals in the gas phase [3]. The existence of this metal–nonmetal transition at the surface has led to the theoretical prediction of an oscillatory electron density profile normal to the surface, commonly referred to as surface induced layering [2,3]. For dielectric liquids on the other hand, the nature of the interactions does not change significantly across the liquid–vapor interface. Theoretical modeling and molecular dynamics studies result in an interfacial density profile that varies monotonically from the bulk liquid density to the vapor density [4,5]. In this paper we review experimental results that unambiguously confirm the existence of surface induced layering for liquid Hg [6], Ga [7] and In [8].

In principle, the surface structure of an elemental liquid metal can be modified by: (i) alloying with a second liquid metal, (ii) physical adsorption and (iii) chemical reaction. The distinction between physical adsorption and chemical reaction at the surface is not defined sharply and is made on the basis of the strength of the bonds formed [9]. Covalent bonds that are formed in chemical reactions have specific stoichiometry and directionality with typical bond strengths ranging from 200 to 900 kJ/mol [9]. By contrast, physical

* Corresponding author. Tel.: +1 617 495 3214; fax: +1 617 495 9837; e-mail: pershan@deas.harvard.edu

0022-3093/99/$ – see front matter
PII: S0022-3093(99)00226-4

adsorption lacks the stoichiometry and directionality of covalent bonds and the bond strengths are around 50 kJ/mol [9]. Alloying of two liquid metals can lead to either non-directional metallic bonds or directional bonding, depending on the interactions between the two types of atoms [10]. In regular alloys, the interactions between the two components are comparable to the interactions between the atoms of each component and the bulk structure is only slightly affected by alloying [10]. This, however, is not necessarily true for the structure of the surface where small differences in these interactions can lead to significant differences between the surface tensions of the two liquid metals. Since surface segregation of the component with smaller surface tension is expected for binary mixtures in general [5], both the surface composition and surface structure may be changed drastically by alloying [10]. If the interactive energies between the two components of the alloy are larger than the cohesive energies between the atoms of the pure components, associated alloys form [10] displaying both directional bonding and well-defined stoichiometry. The effect of this association in the bulk phase on the surface structure of LM has not yet been investigated, but in the case of solid alloys recent results have shown both directional bonding and a mesoscopic segregation profile induced by the surface [11,12]. On the other hand, if the cohesive interactions are stronger than the interactions between the two components, a miscibility gap with a pertinent critical consolute point forms in the bulk phase. Surface wetting effects associated with this bulk phase critical point have been predicted and studied for dielectric liquids [13,14], but at the moment only few experimental studies of these phenomena exist for liquid metals [15–17].

In this review, we discuss how surface-specific X-ray studies can be used to understand the microscopic structure of LM surfaces, how this structure is affected by bulk properties such as the degree of localization of the free electrons and how oxidizing a LM changes its surface structure. In addition, we present experimental studies on binary liquid alloys where important parameters such as size, valence and degree of covalency can be tuned.

2. Theoretical background

The scattering geometry shown in Fig. 1 defines the liquid surface to be lying in the x–y plane, with X-rays incident at an angle α and collected by the detector at a reflection angle β and azimuthal angle 2θ. For liquid surfaces, the momentum transfer $\vec{q}$ is conveniently decomposed into components q_z normal to the surface and q_{xy} lying in the surface plane, which are related to the scattering angles by

$$q_z = \frac{2\pi}{\lambda}(\sin\beta + \sin\alpha) \text{ and } q_{xy} = \frac{2\pi}{\lambda}\sqrt{\cos^2\alpha + \cos^2\beta - 2\cos\alpha\cos\beta\cos 2\theta}.$$

The specular X-ray reflectivity (XR) is defined by $\alpha = \beta$ and $2\theta = 0$. The density profile normal to the surface can be extracted from the measured q_z dependence of the XR. Diffuse scattering (DS) is measured at fixed α for varying β and depends explicitly on both the q_z and the q_{xy} component. DS probes the height fluctuations of the surface.

The theoretical Fresnel reflectivity from an ideally flat and abruptly terminated surface is known from classical optics [18]:

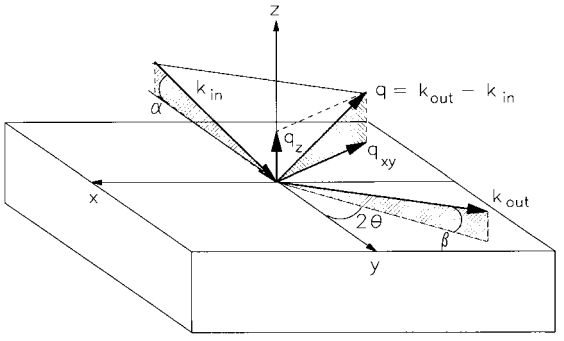

Fig. 1. Sketch of the geometry of X-ray scattering from the liquid surface with the incoming and outgoing angles α and β, the incoming and outgoing wavevector $\vec{k}_{in}$ and $\vec{k}_{out}$, respectively, and the azimuthal angle 2θ. The momentum transfer $\vec{q}$ has an in-plane component q_{xy} and a surface-normal component q_z.

$$R_{\mathrm{f}}(q_z) = \left| \frac{q_z - \sqrt{q_z^2 - q_{\mathrm{c}}^2}}{q_z + \sqrt{q_z^2 - q_{\mathrm{c}}^2}} \right|^2 \approx \left(\frac{q_{\mathrm{c}}}{2q_z} \right)^4 \quad \text{for } q_z \gtrsim 5q_{\mathrm{c}}, \tag{1}$$

where q_{c} is the critical wavevector for total external reflection (typically ~ 0.05 Å^{-1} for metals). To describe scattering from a real surface, the reflectivity from an ideal surface has to be modified in two ways. First, to take into account the structure along the normal to the surface, the Fresnel reflectivity, $R_{\mathrm{f}}(q_z)$, has to be multiplied by a surface structure factor $|\Phi(q_z)|^2$

$$\Phi(q_z) = \frac{1}{\rho_\infty} \int_{-\infty}^{+\infty} \frac{\mathrm{d}\tilde{\rho}(z)}{\mathrm{d}z} \exp(\mathrm{i}q_z z)\, \mathrm{d}z, \tag{2}$$

with the local or intrinsic density profile, $\tilde{\rho}(z)$, and the bulk electron density, ρ_∞. Second, in the case of a real liquid surface, thermally excited capillary waves induce a phase shift between X-rays reflected from different points, r_{xy}, on the surface [19,20]. As shown elsewhere [8], the properly normalized differential cross section, $\mathrm{d}\sigma/\mathrm{d}\Omega$, for the scattering off a thermally roughened liquid surface is given by

$$\frac{\mathrm{d}\sigma}{\mathrm{d}\Omega}(\vec{q}) = \frac{A_0}{\sin\alpha} \left(\frac{q_{\mathrm{c}}}{2} \right)^4 \frac{k_b T}{16\pi^2 \gamma} |\Phi(q_z)|^2 \frac{1}{q_{xy}^2} \left(\frac{q_{xy}}{q_{\max}} \right)^{\eta}, \tag{3}$$

with

$$\eta = \frac{k_b T}{2\pi\gamma} q_z^2, \tag{4}$$

where $(A_0/\sin\alpha)$ is the sample area illuminated by a beam of cross sectional area A_0 and γ is the surface tension. The large wavevector cutoff, $q_{\max} \simeq \pi/a$, where a is the particle size, accounts for the fact that fluctuations with a wavelength shorter than half the particle size are included in $\tilde{\rho}(z)$ [8]. Eq. (3) describes the $\vec{q}$ dependence of both reflectivity and thermal diffuse scattering. The specularly reflected intensity is obtained by integrating Eq. (3) over the solid angle defined by the detector opening when it is centered at $q_{xy} = 0$:

$$R(q_z) = \frac{1}{A_0} \int_{\mathrm{det}} \left(\frac{\mathrm{d}\sigma}{\mathrm{d}\Omega} \right) \frac{\mathrm{d}\Omega}{\mathrm{d}^2 q_{xy}}\, \mathrm{d}^2 q_{xy}. \tag{5}$$

Although the magnitude of the structure factor, $|\Phi(q_z)|$, can be calculated from the measured reflectivity, the phase information is lost and a simple inversion of Eq. (2) to obtain $\tilde{\rho}(z)$ is not possible. Instead, the common procedure is to assume a physically realistic model for $\tilde{\rho}(z)$. Then $\Phi(q_z)$ is calculated according to Eq. (2) and the parameters of the model are varied until the best fit to the data is obtained. One model that has been applied to elemental liquid Hg, Ga and In is to assume a semi-infinite array of layers of variable electron density parallel to the surface. These layers represent planes of metal atoms separated by a distance, d. Mathematically, each layer is represented by a Gaussian whose integral is constrained to the average density of the liquid and whose width increases with increasing distance from the surface. This increasing width models the decrease of the amplitudes of the layers away from the surface [8,21]. To describe the surface structure of alloys, this model must be modified to allow for concentration variations from layer to layer [15,21]. The effect of the thermal fluctuations of the surface height is taken into account by convolving this model for $\tilde{\rho}(z)$ with the capillary wave model for the height distribution of the surface [8,19,20,22].

3. Experimental procedure

3.1. Liquid spectrometer

The large dynamic range in X-ray intensity required to study the structure of the surface of liquids with Å-scale resolution is only accessible by using synchrotron X-ray sources. All experiments reported here have been performed at beamlines X22B and X25 at the National Synchrotron Light Source at Brookhaven National Laboratory. The size of the incoming beam is determined by slits located upstream of a crystal that deflects the synchrotron X-ray beam downward onto the horizontal liquid surface. The X-ray wavelengths

are 0.653 Å (X25) and 1.24 Å (X22B). The X-ray beam enters and exits the ultra high vacuum (UHV) chamber containing the LM sample through Be windows. This chamber is mounted on an active vibration isolation table that effectively quenches mechanical vibrations [8]. The experimental resolution is primarily defined by slits in front of the detector located about 600 mm downstream of the sample. The resolution varies for different experimental configurations. For specular reflectivity, typical slit settings were 4 mm horizontally × 4 mm vertically corresponding to a q_z resolution of about 0.06 Å^{-1}. To record the diffuse scattering, typical slit settings were 4 mm horizontally × 1 mm vertically resulting in a q_z resolution of 0.017 Å^{-1}. For XR and DS experiments, the signal originating from the surface was separated from the background, mostly diffuse scattering from the bulk liquid, by subtracting intensities measured with the detector moved approximately 0.4° out of the reflection plane [8,21].

3.2. Sample preparation

To study the intrinsic properties of the surface of LM, alloys and reacted LM surfaces, it is crucial to maintain a microscopically clean surface. For LM or alloys with a low vapour pressure, this is accomplished by containing the sample in a UHV chamber at a vacuum in the 10^{-10} Torr range. In this case, the formation time for a monolayer of any impurity, most notably oxygen, is much longer than the time necessary to conduct the experiment [23]. Any oxide that is present at the beginning of the experiment when the metal is exposed to air while being transferred into the UHV chamber, was removed by Ar^+ sputtering [8,21]. Controlled oxidation of the LM sample was obtained by exposing the sample to dry oxygen introduced into the UHV chamber through a bakeable leak valve. The oxygen dosage was monitored by a residual gas analyzer and an ion gauge [24]. The preparation of a clean LM alloy surface is described in a separate paper [15]. To study liquid Hg or any of its alloys, a pseudo-UHV approach has to be used since the vapor pressure of liquid Hg is too large to allow the use of standard UHV techniques [25].

4. Results

4.1. The surface of elemental liquid metals

The experimentally determined specular reflectivities from liquid Hg (open circles) [6,25] liquid Ga (closed circles) [7] and liquid In (closed squares) [8] are compared in Fig. 2. These reflectivities are normalized to the theoretical Fresnel reflectivity, R_f, of the pertinent LM. Any deviation from $R/R_f = 1$ indicates the presence of surface roughness or structure normal to the surface. At the smallest q_zs the measured reflectivity indeed coincides with the Fresnel reflectivity from an ideal surface. With increasing q_z, however, the reflectivity deviates from the Fresnel R_f for an ideal surface. The reflectivities from the surface of all three LM investigated so far show maxima centered at 2.5 Å^{-1} (Ga) and 2.2 Å^{-1} (Hg and In). An analysis of the surface structure of these LM based on the density profile calculated from these reflectivities is given in Section 5.1.

4.2. Modified liquid metal surfaces

The normalized reflectivity of a Ga–In alloy with 16.5 at.% In at room temperature is shown in Fig. 3 (closed squares). It can be seen that the Ga layering peak is shifted to a smaller q_z (compare to the reflectivity from elemental Ga represented by open squares in Fig. 3) and also diminished in magnitude. In addition, the reflectivity from the Ga–In surface is greater than the theoretical Fresnel reflectivity for an ideal Ga–In surface at small and intermediate q_zs. Alloying just 0.3 at.% Bi to liquid Ga [26] results in an even larger modification of the room temperature surface structure of liquid Ga (see closed circles in Fig. 3). The Ga layering peak is only discernible as a kink in the reflectivity and is shifted to even smaller q_zs. The reflectivity is almost completely dominated by a broad maximum centered at around 1.2 Å^{-1}.

A comparison of the reactions of the three LM Hg, Ga and In to oxygen is shown in Fig. 4. The

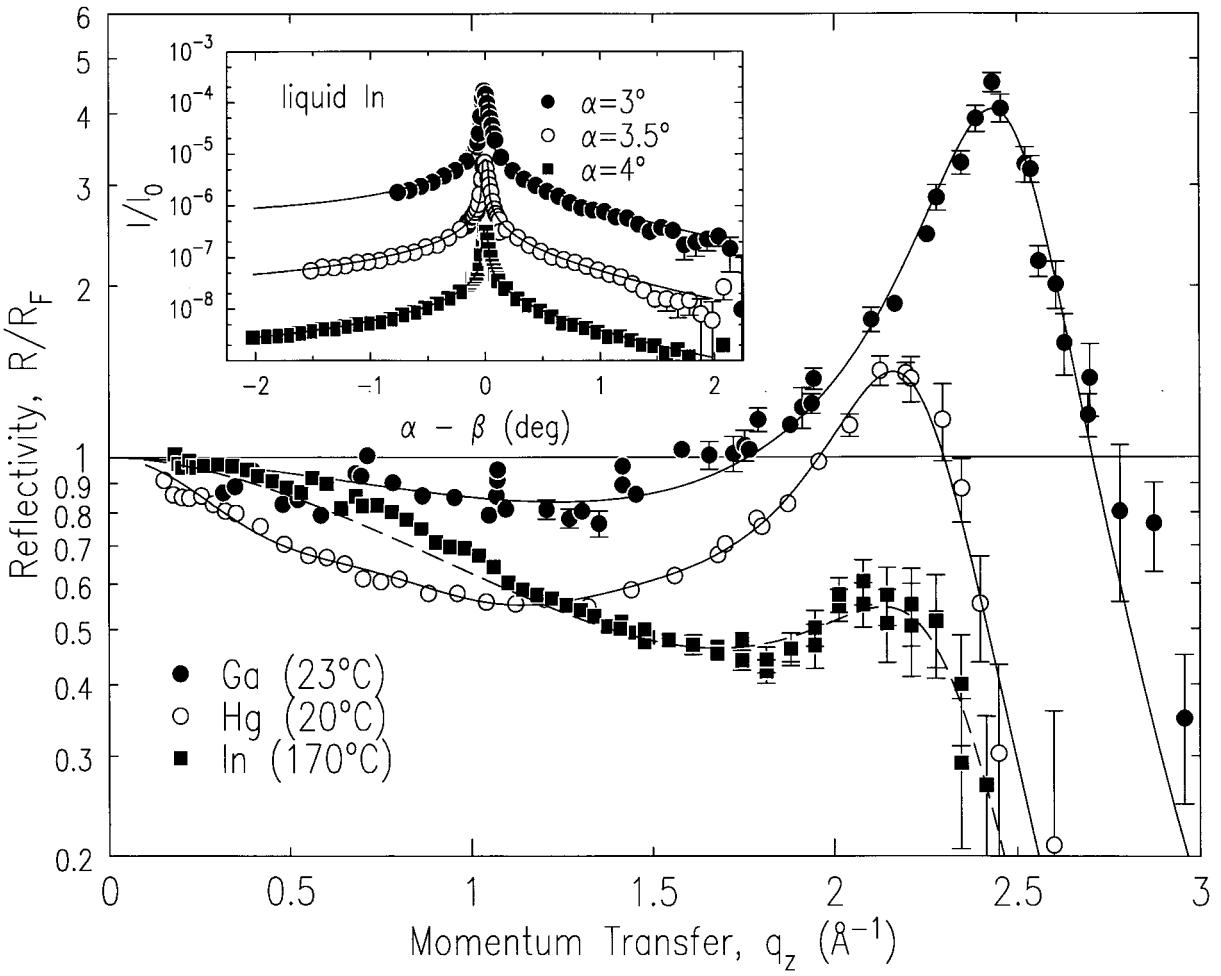

Fig. 2. Reflectivity from liquid Hg at 20°C (open circles), liquid Ga at 23°C (closed circles) and liquid In at 170°C (closed squares) normalized to the Fresnel reflectivity of the respective liquid metal. The solid lines represent the fit of the reflectivity to a Gaussian model for the density with three (Ga, In) or six (Hg) free parameters describing the surface layering. Inset: Diffuse scans in the reflection plane for liquid In for different incident angles α. Integration of these diffuse scans over the resolution volume yields the reflectivity shown in the main figure. For clarity the diffuse scans are multiplied by an arbitrary factor (closed circles: $\times 1000$, open circles: $\times 100$, closed squares: $\times 10$). The solid lines in the inset represent the diffuse scattering calculated from the the general cross section discussed in the text, using the fitted density profile model.

reflectivities are normalized to the Fresnel reflectivity of the pertinent elemental LM. Obviously, the surface of the three metals is affected differently by the presence of oxygen in the gas phase. Both Ga and In have been exposed to the same amount of oxygen (≈ 200 L). The oxygen exposure is expressed in Langmuirs (1 L $= 10^{-6}$ Torr s) which is the dosage that would result in the formation of a monolayer assuming a sticking coefficient of unity for the atoms on the surface [23]. Oxidation of liquid Ga (closed circles in Fig. 4) leads to oscillations whose amplitude does not decay over the measured range of q_z [24]. Indium has a completely different reflectivity (closed squares in Fig. 4; the solid line is a guide to the eye) [8]. The In reflectivity does not change upon exposure to small amounts of oxygen but the formation of macroscopically thick oxide islands on the rim of the sample is visible to the eye. With increasing oxygen exposure, these islands grow inhomogeneously

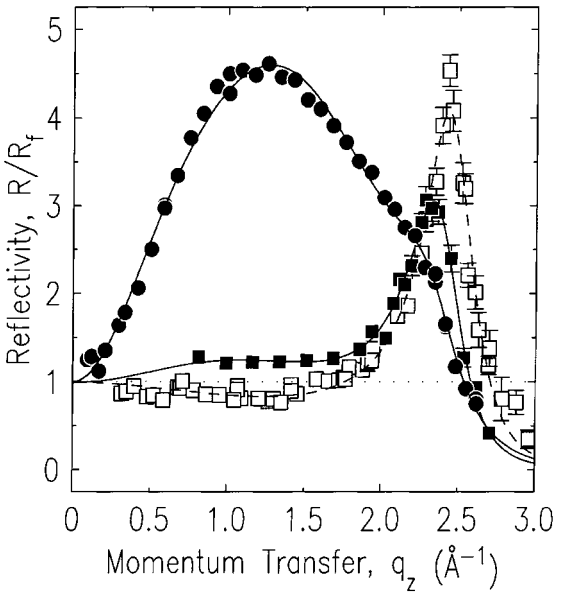

Fig. 3. Reflectivity from the surface of liquid Ga (open squares), liquid Ga–In with 16.5 at.% In (closed squares) and liquid Ga–Bi with 0.3 at.% Bi (closed circles). The reflectivities are normalized to the ideal Fresnel reflectivity of Ga, Ga–In and Ga–Bi, respectively. The dashed line represents the best fit of the Ga reflectivity to a simple Gaussian model describing the surface-induced layering for elemental Ga and the solid lines represent the best fit of the Ga–In and Ga–Bi reflectivity to the same model plus an additional high density surface adlayer.

into the part of the sample that is illuminated by the X-rays and at that point the reflectivity falls steeply with q_z indicating that the surface has become much rougher. Finally, preliminary data are presented on the oxidation of liquid Hg. Due to the high Hg vapor pressure, these experiments have not been conducted in a controlled UHV environment and it was not possible to measure the oxygen partial pressure in the chamber. However, the amount of oxygen in the chamber is comparable to that of the two experiments described above. The reflectivity (closed triangles in Fig. 4) shows oscillations decaying with increasing q.

5. Discussion

5.1. Elemental liquid metals

To calculate the local density profile of LM from the reflectivity shown in Fig. 2, the surface

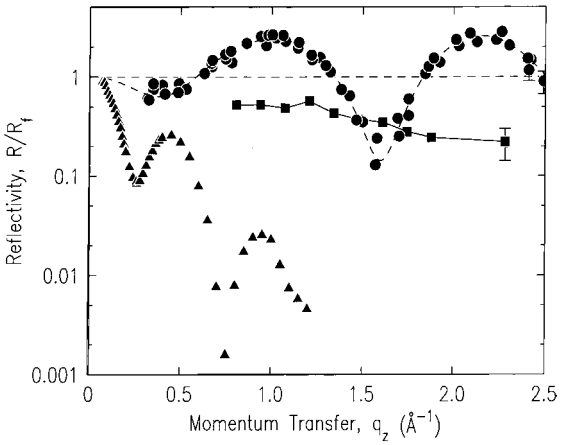

Fig. 4. Reflectivity from the surface of oxidized liquid Ga (closed circles, 200 L oxygen), oxidized liquid In (closed squares, 240 L oxygen) and oxidized liquid Hg (closed triangles, comparable oxygen dosage) normalized to the ideal Fresnel reflectivity of the pertinent pure liquid metal. The dashed line represents the fit of the oxidized Ga reflectivity to a model taking into account the Ga subphase and the oxide film. The solid line through the oxidized In data is only a guide to the eye.

structure has to be deconvolved from the thermally induced height fluctuations. This is only possible, however, when it can be shown that the surface roughness is described by thermally excited capillary waves. We employed two different approaches to demonstrate that the surface roughness of liquid Ga and In can be accurately described by the capillary wave model. The reflectivity of liquid Ga was measured with a single resolution for different temperatures between 22°C and 160°C and all of the data were simultaneously fit to the same model for $\tilde{\rho}(z)$ of Ga convolved with capillary waves having a known temperature dependence [27]. The agreement between the data and these fits was the first evidence that the capillary wave model fully accounts for the roughness of a LM surface. A different approach has been used to show that the same is true for liquid In [8]. Here, the specular reflectivity was only measured for a single temperature; however, at that temperature the diffuse scattering was measured for a number of different angles of incidence (see inset of Fig. 2). Both the specular reflectivity and diffuse scattering were fit to a single model for $\tilde{\rho}(z)$ convolved with capillary waves. As can be seen from

fits to the In reflectivity data in Fig. 2, and to the diffuse scattering from In in the inset, the model describes the experimental data well within their statistical error. Since the only adjustable parameters of the theoretical model (see Eq. (3)) are those necessary to describe the surface structure factor, this capillary wave model indeed describes the roughness of the surface properly. There is now mounting evidence that the capillary wave model completely describes the surface roughness of a variety of liquids; however, it is also clear that for inhomogeneous liquid surfaces the capillary wave model is not adequate. Separate experiments on organic monolayers on water in which the agreement with the capillary wave model is destroyed by compressing the monolayer past the point of elastic stability is an example for this. Inhomogeneities in the compressed monolayer give rise to excess diffuse scattering [22].

Using the deconvolution of the height fluctuations which has been shown to be justified in the case of liquid Ga and In and the simple Gaussian model mentioned above, it is possible to calculate and compare the local density profile for both liquid Ga and In [8]. We find that the amplitude of the electron density of the first layer of In and Ga are essentially identical, although the layering amplitude decays faster for liquid In than for Ga with increasing distance from the surface. Furthermore, the surface layering decay length is comparable to the bulk density pair correlation length in the case of liquid In. By contrast, the layering decay length is considerable larger than the bulk correlation length in the case of liquid Ga. These differences in the surface structure are likely related to the differences in the electronic structure of the bulk phase. For liquid In, virtually all conduction electrons are delocalized and In is considered to be a nearly free electron (NFE) type liquid metal [28,29]. For liquid Ga on the other hand, the conduction electrons are partially localized in covalent bonds [30,31]. The partial covalent bonding in the liquid seems to stabilize surface layering and to expand the distance between the surface layers beyond that expected for simple isotropic hard sphere liquids [8].

It has not yet been possible to compare the intrinsic or local density profile of the Hg surface with the Ga or In surface structure. This problem is due to the experimental observation that the temperature dependence of the reflectivity of liquid Hg cannot be explained by capillary waves alone. This discrepancy indicates that the surface structure of liquid Hg has a temperature dependent component in addition to capillary wave roughening. This unexpected result is discussed in detail elsewhere [25].

5.2. Modified liquid metal surfaces

The effect of alloying liquid Ga with In is shown in Fig. 3. We observe three main differences between the reflectivity from liquid Ga and liquid Ga–In with 16.5 at.% In: (i) the reflectivity at intermediate q_zs, $0.75 \lesssim q_z \lesssim 2.0$, is about 30% larger than the reflectivity from elemental Ga; (ii) the Ga layering peak is shifted to a q_z that is about 15% smaller than that found for elemental Ga; and (iii) the peak amplitude is reduced. All of these effects can be explained by making only one important change to the model used for elemental Ga: a high density surface adlayer is added on top of the layered Ga surface [15,21]. According to the Gibbs adsorption rule from classical thermodynamics this surface segregation is expected since the surface tension of In (556 dyn/cm) is less than that of Ga (718 dyn/cm). Also, the experimental finding that In only segregates into the first layer and the next layer already has the bulk the Ga–In composition is consistent with molecular dynamics simulations for this system [32]. The differences between the X-ray reflectivity from elemental Ga and the Ga–In eutectic are discernible but the Ga layering peak still dominates the reflectivity. This is due to the fact that the electron density of In is only about 5% larger than that of Ga.

In contrast to Ga–In, alloying a very small amount of Bi (0.3 at.%) to liquid Ga results in a larger modification of the surface structure since the electron density difference between Ga and Bi amounts to 50%. The size difference between Bi and Ga (20%) is also larger than that between In and Ga (13%) resulting in the Ga layering peak being shifted to smaller q_zs compared to Ga and Ga–In. The layering is suppressed even more than in the case of Ga–In and is discernible only as a

kink in the reflectivity. The surface structure is dominated by a large and broad maximum that is evident already at the lowest q_zs. Just as for Ga–In, the increase of the measured reflectivity above the theoretical Fresnel reflectivity indicates the segregation at the surface of a species with higher density than the Ga–Bi bulk. Using the same model that was employed for Ga–In yields the same result of a high density monolayer, in this case almost pure Bi, in the uppermost surface layer followed by a subphase with the nominal Ga–Bi alloy concentration [15]. This profile, however, is an adequate description of the reflectivity only at temperatures below the monotectic temperature of the alloy of 222°C. Above this temperature, a wetting phase transition takes place [16] and a thicker Bi-rich film forms [15]. The unexpectedly complicated microscopic structure of this wetting film will be addressed in a forthcoming publication.

A different approach to modify the surface structure of LM is to chemically react the surface. A reaction of great practical importance is to expose a LM to a controlled amount of oxygen. Oxidation of liquid Ga (closed circles in Fig. 4) leads to oscillations indicating the formation of a 5 Å thick oxide film as inferred from the period of these oscillations [24]. Once the oxygen dosage reaches about 400 L, the reflectivity does not change upon further exposure of the LM to oxygen. This indicates that the oxide film is homogeneous and protects the bulk liquid Ga from further oxidation. In addition, the reflectivity was measured as a function of temperature at an oxygen dosage of about 400 L. In this case, the reflectivity does not change with temperature indicating that the 5 Å thick oxide film is solid and therefore quenches capillary waves at the surface. All of the above findings are confirmed by the analysis of the density profile. The model for this profile again incorporates the semi-infinite sum of Gaussians to describe liquid Ga. In addition, a single box of constant density is invoked to describe the oxide film (the dashed line in Fig. 4 depicts the best fit of this model to the data). The fit yields a thickness of 4.9 ± 0.1 Å for the oxide film and a coverage of $85 \pm 1\%$. Virtually the same results are obtained using a more sophisticated model taking the Ga_2O_3 structure into account [24]. Indium reacts in a completely different way upon exposure to oxygen (closed squares in Fig. 4; the solid line is a guide to the eye) [8]. Here, macroscopically thick oxide islands, visible to the eye, are formed [8]. Upon reaching the beam-illuminated area, these islands cause a decrease and temporal fluctuations in the reflectivity rendering further experiments impossible. The data for oxidized Hg (closed triangles in Fig. 4) show oscillations with q_z, indicating a uniform 12 Å thick oxide film. This homogeneous film formation is similar to the one found for oxidized Ga with the exception that the Hg oxide film appears to be rougher since the oscillations decay faster with increasing q_z.

Another approach to modify a LM surface is to spread an organic monolayer on the surface. We found that well defined alkanethiol monolayers and multilayers can be self assembled on the surface of Hg [33,34]. Even though a covalent bond forms between the thiol of the organic molecule and the Hg, the surface layering of the Hg subphase remains unaffected. Organic monolayers on a liquid metal are an interesting example of how the interactions between a surface film and the LM can be modified. Depending on the strength ratio of the chain–chain interaction to the headgroup-substrate interaction, the monolayer ordering can be dominated either by van der Waals like (physical) or strong directional (chemical) interactions. Future studies of thin films on liquid metals for molecules ranging from simple alkanes to complex proteins, some of which do not spread on any other liquid, may provide important information on nucleation and crystallization in two and three dimensions.

6. Conclusions

We have found, and studied, surface induced layering for three liquid metals, Hg Ga and In. Differences in the surface structure of liquid In and Ga can be explained by a different degree of covalency in the bulk liquid phase. Surface oxidation of Ga and Hg yields a homogeneous, uniform thin oxide film whereas macroscopic oxide islands form on liquid In. We have also investigated surface

segregation and surface phase transitions in liquid binary alloys. Surface segregation obeying Gibb's adsorption rule is found for Ga–In and Ga–Bi. In Ga–Bi, however, a wetting phase transition is also found to occur once the alloy is heated past its monotectic temperature.

Future studies will explore the surface behavior of liquid alloys which form various intermetalic phases in the solid bulk and the possibility of surface-stabilization in liquid alloys of ordered phases observed normally in the solid only.

Acknowledgements

This work has been supported by the US Department of Energy Grant No. DE-FG02-88-ER45379, the National Science Foundation Grant No. DMR-94-00396 and the US–Israel Binational Science Foundation, Jerusalem. Brookhaven National Laboratory is supported by US DOE Contract No. DE-AC02-98CH10886. HT acknowledges support from the Deutsche Forschungsgemeinschaft.

References

[1] A. Paskin, in: P.D. Adams, H.A. Davies, S.G. Epstein (Eds.), The Properties of Liquid Metals, Taylor and Francis, London, 1967.
[2] S.A. Rice et al., Adv. Chem. Phys. 27 (1974) 543.
[3] R. Evans, M. Hasegawa, J. Phys. C 14 (1981) 5225.
[4] F.F. Abraham, Rep. Prog. Phys. 45 (1982) 1113.
[5] J.S. Rowlinson, B. Widom, Molecular Theory of Capillarity, Clarendon, Oxford, 1982.
[6] O.M. Magnussen, B.M. Ocko, M.J. Regan, K. Penanen, P.S. Pershan, M. Deutsch, Phys. Rev. Lett. 74 (1995) 4444.
[7] M.J. Regan, E.H. Kawamoto, S. Lee, P.S. Pershan, N. Maskil, M. Deutsch, O.M. Magnussen, B.M. Ocko, L.E. Berman, Phys. Rev. Lett. 75 (1995) 2498.
[8] H. Tostmann, E. Dimasi, P.S. Pershan, B.M. Ocko, O.G. Shpyrko, M. Deutsch, Phys. Rev. B, accepted for publication.
[9] J. Israelachvili, Intermolecular and Surface Forces, Academic Press, London, 1995.
[10] N.H. March, Liquid Metals, Cambridge University, Cambridge, 1990.
[11] C. Ern, W. Donner, A. Rühm, H. Dosch, B.P. Toperverg, R.L. Johnson, Appl. Phys. A 64 (1995) 383.
[12] S. Krimmel, W. Donner, B. Nickel, H. Dosch, C. Sutter, G. Grübel, Phys. Rev. Lett. 78 (1997) 3880.
[13] J.W. Cahn, J. Chem. Phys. 66 (1977) 3667.
[14] S. Dietrich, in: C. Domb, J. Lebowitz (Eds.), Wetting Phenomena, Phase, Transitions and Critical Phenomena, vol. 12, Academic Press, New York, 1986.
[15] H. Tostmann, E. DiMasi, P.S. Pershan, B.M. Ocko, O.G. Shpyrko, M. Deutsch, Ber. Bunsenges. Phys. Chem. 102 (1998) 1136.
[16] W. Freyland, D. Nattland, Ber. Bunsenges. Phys. Chem. 102 (1998) 1.
[17] D. Chatain, P. Wynblatt, Surf. Sci. 345 (1996) 85.
[18] M. Born, E. Wolf, Principles of Optics, Pergamon, Oxford, 1975.
[19] A. Braslau, P.S. Pershan, G. Swislow, B.M. Ocko, J. Als-Nielsen, Phys. Rev. A 38 (1988) 2457.
[20] S.K. Sinha, E.B. Sirota, S. Garoff, H.B. Stanley, Phys. Rev. B 38 (1988) 2297.
[21] M.J. Regan, P.S. Pershan, O.M. Magnussen, B.M. Ocko, M. Deutsch, L.E. Berman, Phys. Rev. B 55 (1997) 15874.
[22] M. Fukuto, R.K. Heilmann, P.S. Pershan, J.A. Griffiths, S.M. Yu, D.A. Tirrell, Phys. Rev. Lett., accepted for publication.
[23] A. Roth, Vacuum Technology, Elsevier, Amsterdam, 1990.
[24] M.J. Regan, H. Tostmann, P.S. Pershan, O.M. Magnussen, E. DiMasi, B.M. Ocko, M. Deutsch, Phys. Rev. B 55 (1997) 10786.
[25] E. DiMasi, H. Tostmann, B.M. Ocko, P.S. Pershan, M. Deutsch, Phys. Rev. B Rap. Commun., accepted for publication.
[26] The Bi content in the liquid Ga–Bi alloy can be varied continuously by changing the temperature as long as an excess of solid Bi is present. In this case, the concentration of Bi in the liquid phase is given by the coexistence curve. A concentration of 0.3 at.% Bi corresponds to a temperature of 35°C.
[27] M.J. Regan, P.S. Pershan, O.M. Magnussen, B.M. Ocko, M. Deutsch, L.E. Berman, Phys. Rev. B 54 (1966) 9730.
[28] B.R. Orton, S.P. Smith, Philos. Mag. 14 (1966) 873.
[29] H. Ocken, C.N.J. Wagner, Phys. Rev. 149 (1966) 122.
[30] A.H. Narten, J. Chem. Phys. 56 (1972) 1185.
[31] A. Bizid, A. Defrain, R. Bellissent, G. Tourand, J. Phys. (Paris) 39 (1978) 554.
[32] S.A. Rice, M. Zhao, Phys. Rev. B 57 (1998) 13501.
[33] O.M. Magnussen, B.M. Ocko, M. Deutsch, M.J. Regan, P.S. Pershan, L.E. Berman, D. Abernathy, J.F. Legrand, G. Grübel, Nature 384 (1996) 250.
[34] M. Deutsch, O.M. Magnussen, B.M. Ocko, M.J. Regan, P.S. Pershan, in: A. Ulman (Ed.), Thin Films: Self-Assembled Monolayers of Thiols, Academic Press, New York, 1998.